

I. I. Bogdanov, V. M. Entov,
and V. P. Stepanov

UDC 536.46

A general mathematical model is proposed for in situ (intrastratum) combustion in a carbonate reservoir on the assumption that it is homogeneous, i.e., does not contain cracks. The efficiency of the thermal decomposition of the rock is estimated from the contribution to the total quantity of carbon dioxide in the mixture at the stratum outcrop. The results of our numerical experiment are compared with preliminary estimates and data from a laboratory experiment on the decomposition of carbonates in furnaces in a stream of nitrogen.†

In situ composition in carbonate reservoirs has a number of distinctive features which are due, on the one hand, to the fracturing inherent to reservoirs of this type and, on the other hand, to the ability of carbonate rocks to decompose and release carbon dioxide, which can affect oil displacement (e.g., [1]).

1. Reaction of Decomposition of Carbonates. The decomposition of limestone, $\text{CaCO}_3 \rightleftharpoons \text{CaO} + \text{CO}_2$, is a typical reaction of the thermal decomposition of carbonate rock (in the presence of one gaseous and one solid reaction product). The reaction is reversible and the equilibrium shifts to the right when the temperature T increases or when the partial pressure p_c of the CO_2 gas in the gas decreases. Data on the dependence of the reaction on the CO_2 reaction are usually given [2].

Suppose that γ is the content of the undecomposed carbonate rock and $\gamma = 1 - \gamma$ is the depth of transformation in the reaction. We write the kinetic relation formally in the form

$$\frac{\partial \gamma}{\partial t} = K(T, p_c - p^*), \quad \gamma > 0, \quad (1)$$

$$\frac{\partial \gamma}{\partial t} = 0, \quad \gamma = 0,$$

where

$$p^* = F(T) \quad (2)$$

is the equilibrium value of the partial pressure of CO_2 at the temperature T . The reaction rate K has the sign of the difference $p_c - p^*$ and may subsequently be larger. This means that we shall consider a process in which local thermodynamic equilibrium is realized at any time:

$$p_c = p^* = F(T). \quad (3)$$

The structure of the thermal wave during in situ combustion in carbonate rocks is usually such‡ that the decomposition zone can be only behind the combustion zone, i.e., higher in the direction of filtration. Even in the absence of combustion the decomposition zone should

†The experiment was performed by S. N. Lykov of the A. P. Krylov All-Union Gas and Oil Scientific-Research Institute, Moscow.

‡Here and below we consider only the single-pass variant of in situ combustion, [3], i.e., combustion with an attendant supply of oxidant: the combustion zone and the external injected mixture move in the same direction.

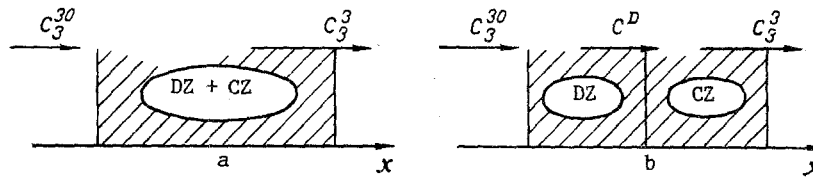


Fig. 1. Possible schemes of the relative position of decomposition and combustion zones.

near the point of maximum temperature of the characteristic profile under consideration, where $K < 0$. Lower along the flow the temperature drops and the conditions for decomposition are lacking since the CO_2 content in the gas exceeds the critical value ($K > 0$). This is especially true when combustion is taken into account since CO_2 is one of its principal products. We should note that lower with respect to the flow the value of the pressure, including p_c , is lower. The temperature dependence of K (or p^*), however, is much more pronounced and the temperature decreases more abruptly than the pressure does; the value of K at the leading edge of the thermal wave, therefore, does not change. The carbonate rock does not undergo reduction here since one of the necessary products (e.g., CaO) is missing.

2. General Equations of the Process. We retain the main concepts of the model of in situ combustion [4, 5], assuming that three-phase ($i = 1$ denotes water, 2 denotes the oil phase, and 3 denotes the gas phase) multicomponent filtration occurs with chemical reactions. First of all we have the standard equations of conservation of phases

$$\frac{\partial (m\rho_i s_i)}{\partial t} + \text{div}(v_i \rho_i) = g_i. \quad (4)$$

Here m is the porosity, ρ_i are the densities of the phases, s_i are the saturations, v_i are the filtrations rates of the phases, and g_i are the densities of the sources for the phases. The aqueous phase contains dissolved carbon dioxide, the oil phase contains a heavy and light oil fractions and carbon dioxide.

We introduce the notation of the component concentrations c_j^i , where i is the number of the phase and j is the number of the component, with $j = 1$ denoting water, 2 denoting the heavy oil fraction, 3 denoting carbon dioxide, 4 denoting oxygen, and 5 denoting the light oil fraction. Disregarding secondary effects we assume that

$$c_1^2 = c_1^4 = c_1^5 = c_2^1 = c_2^3 = c_3^2 = 0.$$

Then we have the equation of conservation of mass for the components

$$\sum_i \left[\frac{\partial}{\partial t} (m\rho_i c_i^j s_i) + \text{div}(\rho_i c_i^j v_i) \right] = q^j, \quad (5)$$

where q^j are the densities of the sources for the components; the diffusion flows are omitted since they are assumed to be small. The heavy oil fraction and oxygen are consumed during combustion while the light oil fraction in the liquid phase is oxidized during low-temperature oxidation [6] (whose thermal effect is disregarded). In accordance with this we put

$$\begin{aligned} q^1 &= \alpha_1 Q + V_1, & q^2 &= \delta P - Q, & q^3 &= \alpha_3 Q - \beta_3 V, \\ q^4 &= -\alpha_4 Q - P, & q^5 &= (1 - \delta) P + V_2, & g_1 &= -V_1, \\ g_2 &= P - Q - V_2, & g_3 &= -g_1 - g_2. \end{aligned} \quad (6)$$

Coefficients α_j and β_j are determined by the stoichiometry of the combustion and the decomposition reaction, δ is determined by the low-temperature oxidation and V_1 and V_2 are the rates of the phase transformations.

The oxidation rate of the fuel will be described by the conventional dependence

$$Q = Z_c \Psi(\rho_3, c_3^1, c_3^2) \exp(-E/RT), \quad (7)$$

where E is the activation energy. The rate of oxygen absorption during low-temperature oxidation is determined by a similar relation

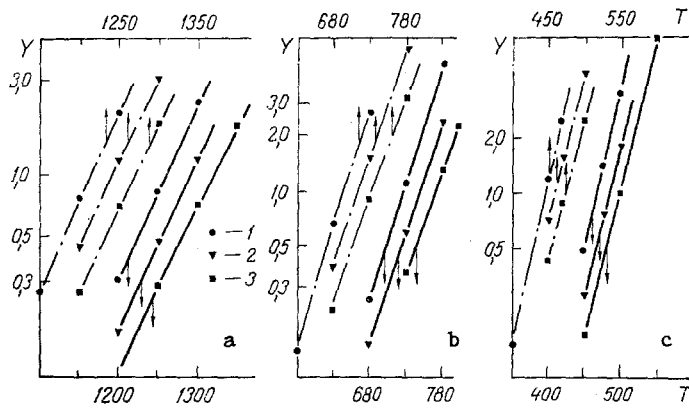


Fig. 2. Lines of the relative contribution of decomposition to the total amount of CO_2 in the gas for different conditions and materials: $p_0 = 3\text{MPa}$ (1), 5(2), 8(3); a) CaCO_3 , b) MgCO_3 , c) FeCO_3 . Temperature T in K.

$$P = Z_0 \Phi(\rho_3, c_3^i) \exp(-U/RT), \quad (8)$$

where U is the activation energy of low-temperature oxidation. In this case $\Psi \sim (\rho_3 c_3^4)^{n_0}$. $(\rho_2 c_2^2)^{n_1}$, $\Phi \sim (\rho_3 c_3^4)^{k_0}$; $\Phi = 0$ if c_3^5 .

When the rate of the convective transfer is rather low, a thermodynamic equilibrium between the liquid phases and their vapor is established in the porous medium. The values of the constants for evaporation and condensation, similar to the value of K (1), are assumed to be so large that whenever $s_1 \neq 0$, $s_2 \neq 0$, and $c_3^5 > 0$ the conditions

$$c_3^i = c_{3*}^i(T, p), \quad (9)$$

are satisfied and the values of s_1 and s_2 are determined by Eqs. (5). We disregard the thermal effect of evaporation of the oil fractions since the thermal effect of the oxidation reaction is much larger.

The flows in all Eqs. (4) and (5) are determined by the generalized Darcy law

$$v_i = -\frac{k_0 f_i}{\mu_i} \nabla p, \quad (10)$$

where p is the pressure for all phases, k_0 is the permeability, f_i are the relative phase permeabilities, and μ_i are the phase viscosities.

The mass balance equations are supplemented by the heat balance equation (on the assumption of local thermal equilibrium):

$$\begin{aligned} \frac{\partial}{\partial t} \{[\gamma \rho_0 c_0 + (1-\gamma) \rho_0^* c_0^*] (1-m) T + m [(\rho_1 c_1 s_1 + \rho_2 c_2 s_2) T + \\ + \rho_3 e_3 s_3]\} + \text{div} [(\rho_1 c_1 v_1 + \rho_2 c_2 v_2) T + \rho_3 v_3 e_3] = \\ = \text{div} (\lambda \text{grad } T) + \chi Q - \chi_c \dot{\gamma}. \end{aligned} \quad (11)$$

Here ρ_0 is the density of the reservoir material and ρ_0^* is the density of the solid decomposition product of the reservoir.

3. Closing Relations. The thermal decomposition of the reservoir material results in a change, generally speaking, in the thermophysical and filtration characteristics of the porous medium. Suppose that the *in situ* combustion is sustained by continuous injection of air with a constant mass flow G . Then in the time t_1 necessary for the combustion zone to traverse a unit length of the stratum ($t_1 = \rho_f \alpha_4 / G a$, where ρ_f is the concentration of the fuel consumed in the reaction and $a = c_3^{4_0}$ is the oxygen content in the air) and the amount of CO_2 obtained from the decomposition of the rock and carried off by the gas flow, is $G(1 + a/\alpha_4) c_3^3 t_1 (1 - c_3^3)$.

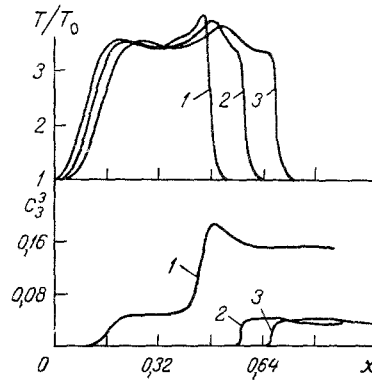


Fig. 3. Computational experiment; distributions of the temperature and the CO₂ fraction in the gas with respect to a dimensionless coordinate (L scale).

For the fraction of the carbonate material subjected to decomposition, therefore, we obtain

$$\eta = \frac{\rho_f c_3^3 \alpha_4 (1 + a_1 \alpha_4)}{(1 - m) \rho_0 a r_c (1 - c_3^3)} \approx \frac{\alpha_4 \rho_f p^*}{(1 - m) \rho_0 a r_3 p_0} \quad (12)$$

Here $r_c = w_3^3/w_0$ and $r_3 = w_3/w_0$. The amount of carbon dioxide obtained from the decomposition of 1 m³ of rock is

$$v = (1 - m) \rho_0 \eta. \quad (13)$$

In actual fact $\eta \ll 1$ and the changes in the thermophysical and filtration characteristics can be disregarded in this approximation.

The carbon dioxide dissolved in the liquid phase affects the density and viscosity of the phases [1]: $\mu_i = \mu_i(c_i^3, T)$ and $\rho_i = \rho_i(c_i^3, T)$, $i = 1, 2$. We assume that the gas phase is subject to the equation of state for an ideal gas, i.e.,

$$\rho_3 = w_3 p / RT, \quad (14)$$

moreover,

$$e_3 = \sum_i c_3^i e_3^i, \quad w_3 = \sum_i c_3^i w_3^i. \quad (15)$$

Analysis shows that when allowance is made for the balance equation of the pore volume

$$\sum_i s_i = 1 \quad (16)$$

and the balance equation for the phase volume

$$\sum_i c_i^j = 1, \quad i = 1 - 3, \quad (17)$$

the system of equations (1) and (4)-(17) is closed.

4. Some Results and Conclusions. The system of equations (1), (4)-(11), and (12)-(17) can be used both as a whole for studying in situ combustion with allowance for all of the factors in it and for assessing the mechanism and role of individual phenomena during thermal effects in the strata. In particular, it was used to verify the estimate of the contribution of thermal decomposition of carbonate rock during in situ combustion to the total carbon dioxide flow. For this purpose we considered the propagation of the heat source in a carbonate reservoir.

Preliminary Estimates. First of all we consider the variant when the zone of intensive thermal decomposition (DZ) that occurs during wet combustion coincides with the combustion zone (CZ) (Fig. 1). The burnup of fuel with mass ρ_f requires a mass $\rho_f z$ of vapor-air mixture; $z = \alpha_4/a(1 - b)$, where $b = c_3^3$ is the mass content of vapor in the gas mixture in the

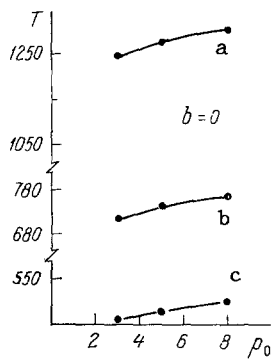


Fig. 4

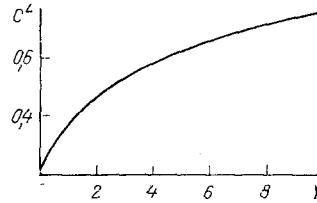


Fig. 5

Fig. 4. Lines of the onset of intensive thermal decomposition in situ combustion: a) calcite, b) magnesite, c) siderite, p_0 = MPa.

Fig. 5. Mass fraction of CO_2 in dry gas mixture at the exit from a stratum [see (27)].

zone of superheated vapor behind the combustion zone. The mass of CO_2 during burnup of fuel in a unit volume of stratum is

$$\rho_c^1 = r_f \rho_f / (1 + \xi). \quad (18)$$

Here $r_f = w_3^3 / w_f$ and the H/c ratio under in situ conditions usually is $n = 1.5-1.8$. The initial CO_2 content c^0 in air and the mass ρ_c^D of CO_2 released during the decomposition of carbonates (per unit volume of stratum) determine the total mass $\rho_{3\Sigma}$ of gas released during the wet in situ combustion and the mass content of CO_2 in it:

$$\rho_{3\Sigma} = (1 + z) \rho_f + \rho_c^D, \quad (19)$$

$$c_3^3 = (\rho_c^0 + \rho_c^1 + \rho_c^D) / \rho_{3\Sigma}, \quad (20)$$

where $\rho_c^0 = \rho_f z_1$ and $z_1 = z(1 - b)$. From this we easily find that the ratio of the masses of CO_2 released during decomposition and combustion is determined by the expression

$$Y = \rho_c^D / \rho_c^1 = \frac{(1 + z)(1 + \xi)}{r_f(1 - c_3^3)} (c_3^3 - c_*). \quad (21)$$

Here

$$c_* = \left(\frac{r_f}{1 + \xi} + c^0 z_1 \right) / (1 + z). \quad (22)$$

Clearly, for decomposition to begin it is necessary that c_3^3 , which is defined by (20), be greater than c_* which is defined by (22). In terms of the pressure this condition is

$$p^* > p_0 \left[1 + \frac{r_s}{c_*} - r_s \right]^{-1}, \quad (23)$$

where $r_s = w_3^3 / w_3^{0*}$.

The decomposition "threshold" c_* is determined, as follows from (22), by the initial CO_2 content in air (which amounts to a mass content of about 0.046%) and the release of carbon dioxide as a product of the combustion.

Decomposition proceeds more intensively by an other scheme, shown in Fig. 1b. The decomposition reaction is localized immediately behind the combustion zone and occurs at virtually the same temperature as, or slightly lower than, in the combustion zone. In this case the quantities ρ_c^1 , $\rho_{3\Sigma}$, c_3^3 , and ρ_c^0 are determined by Eqs. (18)-(20). Instead of (21) we obtain

$$Y = \frac{z(1 + \xi)}{r_f(1 - c^D)} (c^D - c_{**}), \quad (24)$$

*We utilized the fact that during in situ combustion the filtration drops of the pressure are substantially smaller than the reservoir pressure p_0 and we set the pressure in the in situ combustion equal to p_0 .

where

$$c_{**} = (1 - b)c^0, \quad (25)$$

and we must substitute c_{**} for c^* in (23). The quantity $c^D > c_{**}$ determines the CO_2 concentration in the gas ahead of the combustion zone. Equations (21) and (24) can also be written as

$$Y = Y_0 \left[\frac{p^*(1-c)}{p_0 - p^*} - \frac{c}{r_s} \right]. \quad (26)$$

Here $U_0 = A(1 + \xi)r_s/r_f$; $A = 1 + z$, $c = c_*$ for (21), and $A = z$, $c = c_{**}$ for (24). After a quantity $bz\rho_f$ of water vapor entering from the region behind the combustion zone and a quantity $bz\rho_f$ (where $\alpha_1 = nw_1/2w_f$) of water vapor released during combustion condense in a weakly heated zone of the stratum the mass content of CO_2 in the gas mixture (dry) is

$$c^L = \frac{1 + Y + c^0 z_1 (1 + \xi)/r_f}{Y + (1 + z_1 - \alpha_1)/r_f}. \quad (27)$$

Using (22)-(27) as well as the function $p^* = F(T)$, then in the form [7]

$$\lg F = I + BT + 1.75 \log T - \frac{D}{T}, \quad (28)$$

we estimated the efficiency of thermal decomposition during in situ combustion of the following carbonates: a) calcite $D = 9312$ K, $B = 1.096 \cdot 10^{-3}$ K^{-1} , and $I = 0.1171$; b) magnesite $D = 6174$ K, $B = -1.988 \cdot 10^{-3}$ K^{-1} and $I = 4.4648$; c) siderite, $D = 4261$ K, $B = -6.974 \cdot 10^{-3}$ K^{-1} and $I = 7.2488$ (p^* , MPa).

We rewrite (3) as $p^*/p_0 > \varepsilon$, where $\varepsilon = (1 + r_s/c_* - r_s)^{-1}$. For $n = 1.65$, $a = c_3^{4c} = 0.23$, $\alpha_4 = 3.12$, $c^0 = 0.00046$, and $\xi = 0.2$ we obtain $c_* = 0.18$ and $\varepsilon = 0.126$ at $b = \frac{2}{3}B = 0$ and $c_* = 0.093$ and $\varepsilon = 0.052$ at $b = 0.5$. An increase in the fraction of water vapor (the water/air ratio) formally lowers the "threshold" quantity c_* because of a decrease in the oxygen content in the flow and, therefore, in the content of CO_2 (combustion product) in the gas mixture. At $p_0 \sim 2-10$ MPa the characteristic value can be reached at combustion-zone temperatures above 200 K (calcite) and 800 K (magnesite).

Figure 2 shows the graphs of $Y(T)$ plotted in accordance with (26) for three carbonates, whose decomposition constants are given above. The three lowest lines correspond to decomposition in dry air ($b = 0$) and the three upper lines, in moist air ($b = 0.5$).

Computational Experiment. We made a computational study of the thermal decomposition of a heated carbonate material with a purging flow of gas (nitrogen), i.e., we stimulated the conditions of the laboratory experiment. We then studied the propagation of the combustion zone through immobile fuel present in a carbonate reservoir. We assumed that $s_1 = c_2^5 = c_2^3 = 0$ and used the value for $K(T, p_c - p^*)$ measured in the aforementioned experiment. The methodological aspects of the construction of a numerical model (method of fine differences) and variations of the calculations were discussed in detail in [8].

In the calculations we used the following constants: $m = 0.2$, $k_0 = 10^{-12}$ m^2 , $\rho_0 = 2600$ kg/m^3 , $c_0 = 0.84$ kJ/kg , $\lambda = 2$ $W/cm \cdot ^\circ C$, $p_0 = 13$ MPa, $\rho_f = 25$ kg/m^3 , $\rho_g = 900$ kg/m^3 , $c_2 = 1.9$ $kJ/kg \cdot ^\circ C$, $T_0 = 300$ K, $\chi = 4.06 \cdot 10^4$ kJ/kg , $L = 1$ m, and $K = 4.1 \cdot 10^9 \exp(-8130/T) \cdot (1 - p_c/F)w_0$ $kg/m^3 \cdot sec$.

In the first series of calculations we compared the values of c^3 at the exit from the sample with those observed experimentally. There is good agreement in the range of temperature established in laboratory furnaces in the experiment (from 795 to 855°C). In a second series we attempted to determine the temperature in the heat source, during which the decomposition of the given rock becomes considerable in comparison with the formation of carbon dioxide during combustion. Figure 3 shows some results of this series of calculations in the form of distributions of the temperature and the CO_2 fraction in the gas at successive times. Curves 1 correspond to the time when the combustion of fuel was accompanied by thermal decomposition of the rock and curves 2 and 3, after programmed decomposition "switch-off", i.e., we set $K = 0$. We see that a significant contribution is observed at temperature $T \sim 1200$ K. (Calcite formed the basis of the rock studied.)

The results of our numerical calculations indicate that, evidently, some intermediate scheme of arrangement of decomposition and combustion zones is in fact realized (see Fig. 1), with a partial overlap of the zones. The temperature in the combustion zone during decomposition increases since the density (and volume heat capacity) of the porous material decreases.

The fact that the temperature increases makes it possible to estimate the "overlap" of the zones: for the variant given here no less than one-quarter of the total amount of the dissociated material is reacted within the confines of the zone of heat release.

Curves 1 show that decomposition begins substantially higher in the flow in the region of the local temperature maximum formed upon the initiation of the combustion wave. After the decomposition had been "switched off" c_3^3 decreased to a value corresponding to CO_2 outflow during combustion. This value is low in this variant since the oxidant is not used completely in the reaction.

Summarizing the data obtained, we can state the following. Decomposition proceeds more effectively when the reservoir pressure is lower and the temperatures at the heat source of in situ combustion are higher. The temperature dependence in this case is fairly strong and for each substance we can arbitrarily determine the temperature limit of the onset of thermal decomposition [corresponding, e.g., to $Y = 1$ and, generally speaking, specific to each regime of in situ combustion with respect to the value of the water/air ratio, in other words, b in the form of the dependence $T(p_0)$ (Fig. 4)].

The additional CO_2 obtained because of the decomposition somewhat reduces the CO_2 outflow rate and the "slowing down" is more pronounced when the thermal decomposition is more intensive. This is illustrated by the shape of the $c^L(Y)$ curve in Fig. 5, which corresponds to (27); in Fig. 2 the increase in Y for $b = 0.5$ is due to lowering of the relative content of combustion products in the gas (because of the "additional" inflow of water vapor) and not by an intensification of the thermal decomposition. There are no grounds, evidently, for expecting an effect of decomposition from calcite under ordinary in situ decomposition regimes. For reservoirs containing magnesite a significant result can be obtained for strata with $p_0 < 5$ MPa. Siderite can decompose intensively during in situ combustion over a wide range of conditions.

NOTATIONS

Here a , c_3^{40} is the oxygen content in the air (by mass); b , c_3^{2B} is the water vapor content in the gas mixture behind the decomposition zone; c_j^i is the concentration of the j -th component of the mixture in the i -th phase; c_0, c_0^* , and c_1 are the heat capacities of the rock, the solid decomposition product, and the i -th phase; c^0, c_3^{30} is the initial CO_2 content in the air; c^D is the CO_2 content in the gas after the decomposition zone; e_3 and e_3^j are the specific enthalpies of the mixture and the component of the mixture; $n_{0,1}$ and l_0 are the orders of the reactions; L is the size of the computational element of the reservoir; w_i, w_i^j , and w_f are the molecular masses of the i -th phase ($i = 1, 3$), the j -th component in the i -th phase, and an arbitrary unit CH_0 of the fuel; w_3^0 is the molecular mass of the gas mixture without CO_2 (at the exit from the stratum); $Z_{C,0}$ are the preexponential factors in the expressions for the mass rates of combustion and low-temperature oxidation; α_j and β_j are the stoichiometric coefficients for the j -component of the mixture in the combustion and thermal decomposition reactions and δ_j , in the low-temperature oxidation reaction λ is the thermal conductivity; χ and χ_C are the thermal effects of the combustion and decomposition (per kg); and ξ is the ratio of the volume fractions of the combustion products CO and CO_2 .

LITERATURE CITED

1. L. W. Holm and U. A. Josendal, JPT, December, 26, 1427 (1974).
2. R. S. Boynton, Chemistry and Technology of Lime and Limestone, Wiley-Interscience, New York (1963).
3. S. M. Farouq Ali, Production Monthly, 31, No. 11, 4 (1967).
4. B. S. Gottfried, SPE Journal 5, No. 3, 196 (1980).
5. K. H. Coats, SPE Journal, 6, No. 6, 533 (1980).
6. M. K. Dabbous and P. F. Fulton, JPT, June, 26, 253 (1974).
7. M. Kh. Karapet'yants, Chemical Thermodynamics [in Russian], Moscow (1975).
8. I. I. Bogdanov and L. A. Hudov, Dynamics of Multiphase Media [in Russian], Novosibirsk (1980).